Volume 12 | Number 17 | 7 September 2025

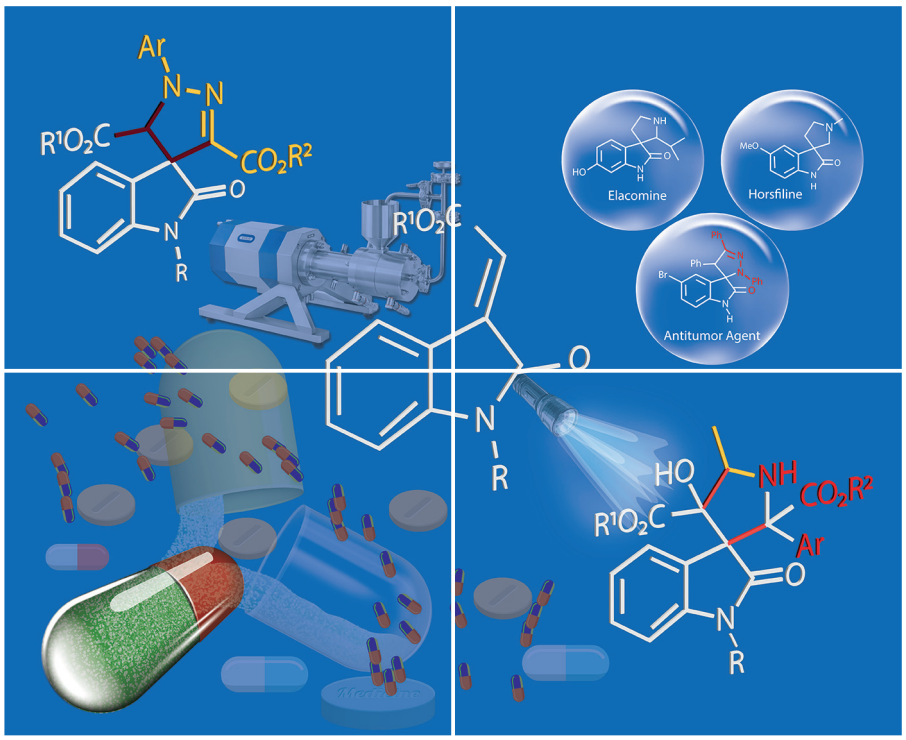

ORGANIC CHEMISTRY

FRONTIERS

CCS 中国化学会 CHINESE CHEMICAL SOCIETY
SIOC 1950
ROYAL SOCIETY OF CHEMISTRY
rsc.li/frontiers-organic

ORGANIC CHEMISTRY FRONTIERS

RESEARCH ARTICLE

View Article Online
View Journal | View Issue

Cite this: *Org. Chem. Front.*, 2025, **12**, 4698

Metal- and base-free spirocyclization of alkylidene oxindoles *via* photo- and mechanochemically-generated nitrile ylides and nitrile imines as 1,3-dipoles†

Shweta Singh,‡[a] Roopam Pandey, ‡[a] Varun Christopher,[a] Mahesh Kumar Ravva, [b] Rakesh Ganguly [a] and Subhabrata Sen *[a]

Received 6th June 2025,
Accepted 11th July 2025

DOI: 10.1039/d5qo00851d

rsc.li/frontiers-organic

Herein we have reported an expedient synthesis of spiro[pyrrolidine-3,3′-oxindole] and 2′-aryl-2′,4′-dihydrospiro[indoline-3,3′-pyrazol]-2-one under metal- and base-free conditions through the 3 + 2 cycloaddition reactions of *in situ* generated nitrile ylides and nitrile imines with alkylidene oxindoles in good to excellent yields. The nitrile ylides are generated through acetonitrile insertion onto carbenes generated from blue LED irradiation of aryl diazo esters. The nitrile imines were formed under mechanochemical conditions from diazo esters and aryl diazonium tetrafluoroborates.

Spirocyclic oxindole scaffolds represent a privileged class of heterocyclic frameworks in medicinal chemistry and materials science.[1] Among them, spiro[pyrrolidine-3,3′-oxindole] and 2′,4′-dihydrospiro[indoline-3,3′-pyrazol]-2-one (spiropyrazoline oxindole) are structurally diverse and biologically significant. Their rigid 3D framework, tunable electronic properties, and wide range of biological applications make them essential in medicinal chemistry, materials science, and organic synthesis. With advancements in asymmetric catalysis, green chemistry approaches, and electrochemical methodologies, their utility continues to expand, reinforcing their role as privileged structures in modern drug discovery and functional materials.[2,3]

The structural and electronic features of these building blocks include a fused indoline-lactam (2-one) system that provides hydrogen-bonding sites and contributes to molecular recognition. The spiro-carbon junction connects the oxindole nucleus to the heterocyclic system, creating steric hindrance and reducing conformational flexibility, which enhances receptor selectivity in bioactive molecules. The spiro[pyrrolidine-3,3′-oxindole] contains a fused pyrrolidine ring, increasing steric hindrance and modulating biological interactions whereas the 2′-aryl-2′,4′-dihydrospiro[indoline-3,3′-pyrazol]-2-one incorporates a pyrazoline moiety, providing electron-rich nitrogen atoms that enhance interaction with biomolecules. These compounds exhibit numerous biological activities including anticancer properties as inhibitors of topoisomerases, kinases, and microtubule polymerization.[4] The spiro-framework enhances bacterial and viral enzyme binding, showing promise as antibiotics and antivirals.[5] They are also used as modulators of CNS receptors resulting in potential anticonvulsant, antidepressant, and neuroprotective effects and as inhibitors of COX-2 enzyme and inflammatory cytokines, making them potential pain-relieving drugs.[6,7] Their application beyond medicinal chemistry includes organic semiconductor photonics.[5] Some of their derivatives enhance guest–host interactions in supramolecular assemblies.[5]

The general synthesis of these spirocyclic frameworks involves a variety of methodologies, including [3 + 2] cycloaddition reactions of azomethine ylides (generated *in situ* from oxindole derivatives) with dipolarophiles (alkenes, alkynes, and nitriles) to construct the spirocycle, multicomponent reactions (MCRs) involving one-pot condensation of isatins, amines, and electron-deficient alkenes, leading to rapid access to spirocyclic products, metal-catalyzed and asymmetric synthesis with chiral Lewis acids and organocatalysts to promote enantioselective transformations, yielding optically pure derivatives, and electro-oxidative and photoredox-mediated reactions, enabling eco-friendly synthesis with enhanced selectivity.[1,8–10]

Nitrile ylides belong to the class of 1,3-dipoles where a carbanionic centre is conjugated with a nitrile group, resulting in structures possessing strong nucleophilic character at the carbon adjacent to the nitrile group, allowing them to participate in cycloaddition reactions and nucleophilic addition

[a]*Department of Chemistry, School of Natural Sciences, Shiv Nadar University Deemed to be University Institute of Eminence, Dadri, Chithera, Gautam Buddha Nagar, UP 201314, India. E-mail: Subhabrata.sen@snu.edu.in*
[b]*Department of Chemistry, SRM University-AP, Amaravati 522240, India*

†Electronic supplementary information (ESI) available. CCDC 2356680. For ESI and crystallographic data in CIF or other electronic format see DOI: https://doi.org/10.1039/d5qo00851d

‡Equal contributors.

reactions.[11] Whereas nitrile imines are a class of 1,3-dipolar species that consist of a conjugated system involving a nitrile group and an imine moiety. Nitrile imines exhibit nucleophilic character at the terminal nitrogen and electrophilic behaviour at the central carbon. This ambident nature makes them highly reactive toward dipolarophiles.[12]

Both nitrile imines and nitrile ylides are highly versatile synthetic intermediates, offering unique electronic properties that allow for regio- and stereoselective functionalization of organic molecules. Their broad applicability in heterocyclic synthesis, medicinal chemistry, and materials science makes them indispensable tools in modern organic synthesis. Nitrile ylides, due to their unique electronic structure, are highly reactive intermediates that participate in diverse reactions, such as [3 + 2] cycloadditions with electron-deficient alkenes or alkynes, leading to aziridines, pyrroles, and other nitrogen-containing fused heterocycles, electrophilic trapping with carbonyl compounds and imines to generate heterocyclic scaffolds relevant to drug discovery,[13,14] and metal-catalysed functionalization with gold(I) or silver(I)-catalysed transformations that introduce complex heterocyclic motifs.[15,16] On the other hand, nitrile imines are widely used in 1,3-dipolar cycloaddition reactions, particularly with electron-deficient alkenes and alkynes.[17] The most notable transformation is their reaction with alkenes to form pyrazoles, an important heterocyclic scaffold in medicinal chemistry.[18] Key reactions involving nitrile imines are cycloaddition with alkenes to pyrazolines, which can be further oxidized to pyrazoles,[19] cycloaddition with alkynes leading to the direct formation of pyrazoles *via* a [3 + 2] mechanism,[17] reaction with isocyanates and isothiocyanates to yield triazolone or thiotriazolones, which have pharmaceutical relevance, and finally, metal-catalysed cross-coupling reactions.[18] Functionalized nitrile imines can participate in transition-metal-catalysed transformations, including palladium- or copper-catalysed coupling with aryl halides.[17]

3-Alkylidene oxindoles are versatile compounds with significant synthetic and biological importance.[20] Their unique structural features facilitate diverse chemical transformations, and their presence in bioactive molecules underscores their potential in drug discovery and development. Ongoing research continues to explore novel synthetic methodologies and applications for these compounds in various therapeutic areas. The exocyclic double bond in 3-alkylidene oxindoles serves as a reactive site for various chemical transformations such as Michael addition reactions with nucleophiles, facilitating the formation of diverse functionalized oxindoles.[21,22] 3-Alkylidene oxindoles can participate in [3 + 3] and [4 + 2] cycloaddition reactions with electrophiles, leading to the construction of complex polycyclic structures.[23,24] Biocatalytic reduction of the alkylidene double bond using baker's yeast has been demonstrated, providing access to 3-alkyl oxindoles with high stereoselectivity.[25]

There are significant advances in the field of photochemical carbene transfer reactions through blue LED-induced transformations of diazo esters. Aryldiazoacetates can undergo efficient photolysis under blue light irradiation (460–490 nm) to generate free carbene intermediates without the need for metal catalysts. These carbenes participate in diverse transformations, including cyclopropanation, C–H insertion, and heteroatom–H insertion reactions, often with high yields and diastereoselectivity. These findings underscore the potential of visible-light photochemistry as a sustainable and practical alternative to traditional metal-catalyzed carbene transfer methodologies.[26–30]

We report the synthesis of densely functionalized spiro[pyrrolidine-3,3′-oxindoles] and 2′-aryl-2′,4′-dihydrospiro[indoline-3,3′-pyrazol]-2-one as diastereomeric mixtures *via* a mild, metal- and base-free [3 + 2] cycloaddition of 3-alkylidene oxindoles with *in situ* generated nitrile ylides and nitrile imines, respectively (Scheme 1). The nitrile ylides are generated under blue LED irradiation of aryl diazo esters followed by nitrile insertion of the resulting carbenes. The cycloaddition product undergoes oxidation to afford the desired compounds. In contrast, the nitrile imines are formed spontaneously through the reaction between ethyl diazoacetate and aryl diazonium tetrafluoroborates under solvent-free mechanochemical ball milling. The target spirocyclic compounds are obtained in

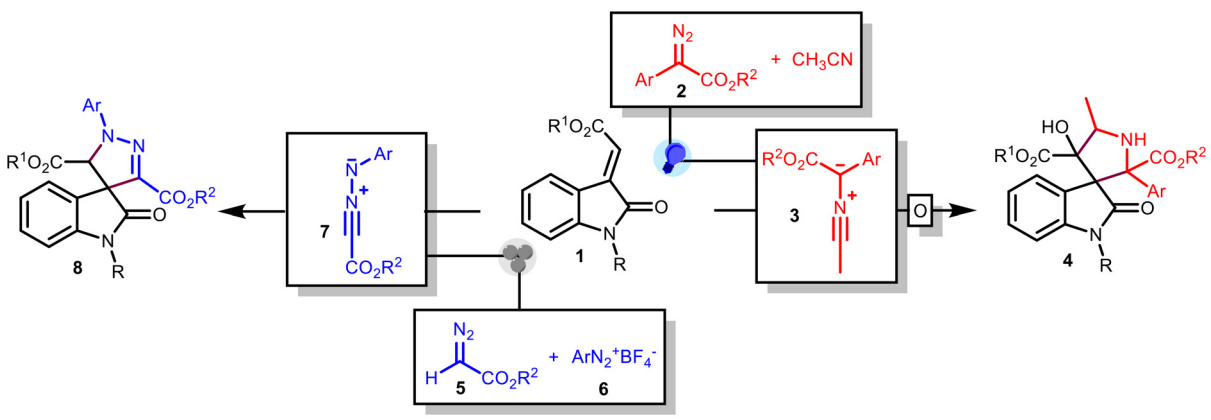

Scheme 1 Summary of our work.

excellent yields under operationally simple and mild conditions (Scheme 1).

These sustainable methods rival traditional thermally-induced and recent metal-catalysed variants, providing operational simplicity, cleaner reaction profiles, and enhanced environmental compatibility.

To initiate our study, we examined the intermolecular [3 + 2] cycloaddition of phenyl diazoacetate **2a** with *tert*-butyl (*E*)-3-(2-ethoxy-2-oxoethylidene)-2-oxoindoline-1-carboxylate **1a** (2 : 1 ratio) in acetonitrile under blue LED irradiation (5 W, 440 nm) at room temperature (Table 1, entry 1). The cycloadduct formed *in situ* was oxidized under ambient conditions to afford spiropyrrolidine-3,3′-oxindole **4a** in 85% yield. Switching to other LED sources—white, red, or green—resulted in lower yields (45–61%) and increased formation (25–30%) of 1,3-oxazole by-products (Table 1, entries 2–4).

Using 15 equivalents of acetonitrile as the nitrile source in alternative solvents such as MeOH, DCE, DCM, TFE, DMF, and acetone either suppressed product formation or yielded only trace amounts of products (2–5%) (Table 1, entries 5–10). Increasing the blue LED intensity from 5 W to 34 W enhanced the yield to 92% (Table 1, entry 11). UVA irradiation afforded **4a** in 73% yield (Table 1, entry 12).

Reactions under nitrogen slowed significantly, giving **4a** in 56% yield with ~40% 1,3-oxazole formation (Table 1, entry 13). Under an oxygen atmosphere, only 2% of **4a** was obtained, with the keto ester as the major product, suggesting that oxygen insertion inhibited ylide formation (Table 1, entry 14).

All reactions were conducted at room temperature. The desired product **4a** was consistently obtained as a diastereomeric mixture (dr 70 : 30 to 80 : 20). Thus, the optimized conditions involve irradiating a 1 : 1 mixture of **1a** and **2a** in acetonitrile with a blue LED (34 W, 440 nM) under open air at room temperature for 8–12 h.

With the optimized conditions in hand (blue LED, 34 W, 450 nm), we next evaluated the scope and robustness of our photolytic protocol using a variety of alkylidene oxindoles **1a–1l** and aryl diazo esters **2a–2j** in acetonitrile at room temperature under open-air conditions (Schemes S1 and S2, ESI†). The desired spiropyrrolidine-3,3′-oxindoles **4a–4r** were obtained in moderate to excellent yields as mixtures of diastereomers (dr = 78 : 28 → 10 : 1) (Scheme 2a).

The alkylidene oxindoles tested included *N*-protected derivatives bearing *tert*-butoxycarbonyl **1a–1f**, acetyl **1g–1h**, methyl **1i**, tosyl **1j**, and benzyl **1k–1l** groups. All were well tolerated under the optimized conditions, affording products in yields ranging from 69 to 92% (Scheme 2a). Among them, Boc-protected substrates performed the best, followed by acetylated analogues, with other protecting groups showing slightly diminished efficiency.

Along with products **4a**, **4f–4h**, **4j**, **4l** and **4o–4q** from phenyl diazo esters, the aryl diazo esters bearing both electron-donating and electron-withdrawing groups at the *para*- and *meta*-positions were also compatible. However, diazo esters with electron-donating substituents at the phenyl ring provided the desired products such as **4b**, **4c**, **4d**, **4e**, **4i**, **4k**, **4n** and **4r** in better yields compared to the electron-withdrawing substituent **4m** (*p*-fluorophenyl). In contrast, *o*-nitrophenyl methyl diazoacetate **2k** failed to deliver the desired product, likely due to the electronic or steric inhibition of ylide formation. All the products were obtained as a mixture of diastereomers (Scheme 2a).

It is noteworthy that to establish the involvement of the nitrile ylide **3** as a dipolarophile, the reaction between **1a** and

Table 1 Optimization for the generation of spiropyrrolidine-3,3′-oxindole **4a**

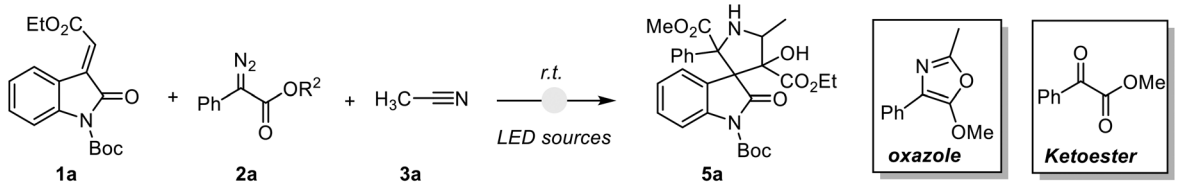

1a 2a 3a 5a

Entry	LED source	Temperature (°C)	Solvent	Yield of **5a** [a] (%)
1	BL (5 W) (440 nm)	rt	ACN	85
2	White	rt	ACN	70
3	Green	rt	ACN	62
4	Red	rt	ACN	40
5	Blue	rt	CH_3CN (15 eq.) + MeOH	0
6	Blue	rt	CH_3CN (15 eq.) + DCE	0
7	Blue	rt	CH_3CN + DCM (15 eq.)	Trace
8	Blue	rt	CH_3CN + TFE (15 eq.)	0
9	Blue	rt	CH_3CN + DMF (15 eq.)	0
10	Blue	rt	CH_3CN + acetone (15 eq.)	0
11	BL (34 W) (440 nm)	rt	CH_3CN	92
12	370 nm UVA	rt	CH_3CN	73
13[b]	BL (34 W) (440 nm)	rt	CH_3CN	56 (40% oxazole)
14[c]	BL (34 W) (440 nm)	rt	CH_3CN	2 (majority keto ester)

[a] Isolated yield. [b] Under nitrogen (N_2). [c] Under an oxygen balloon (O_2); BL: blue LED.

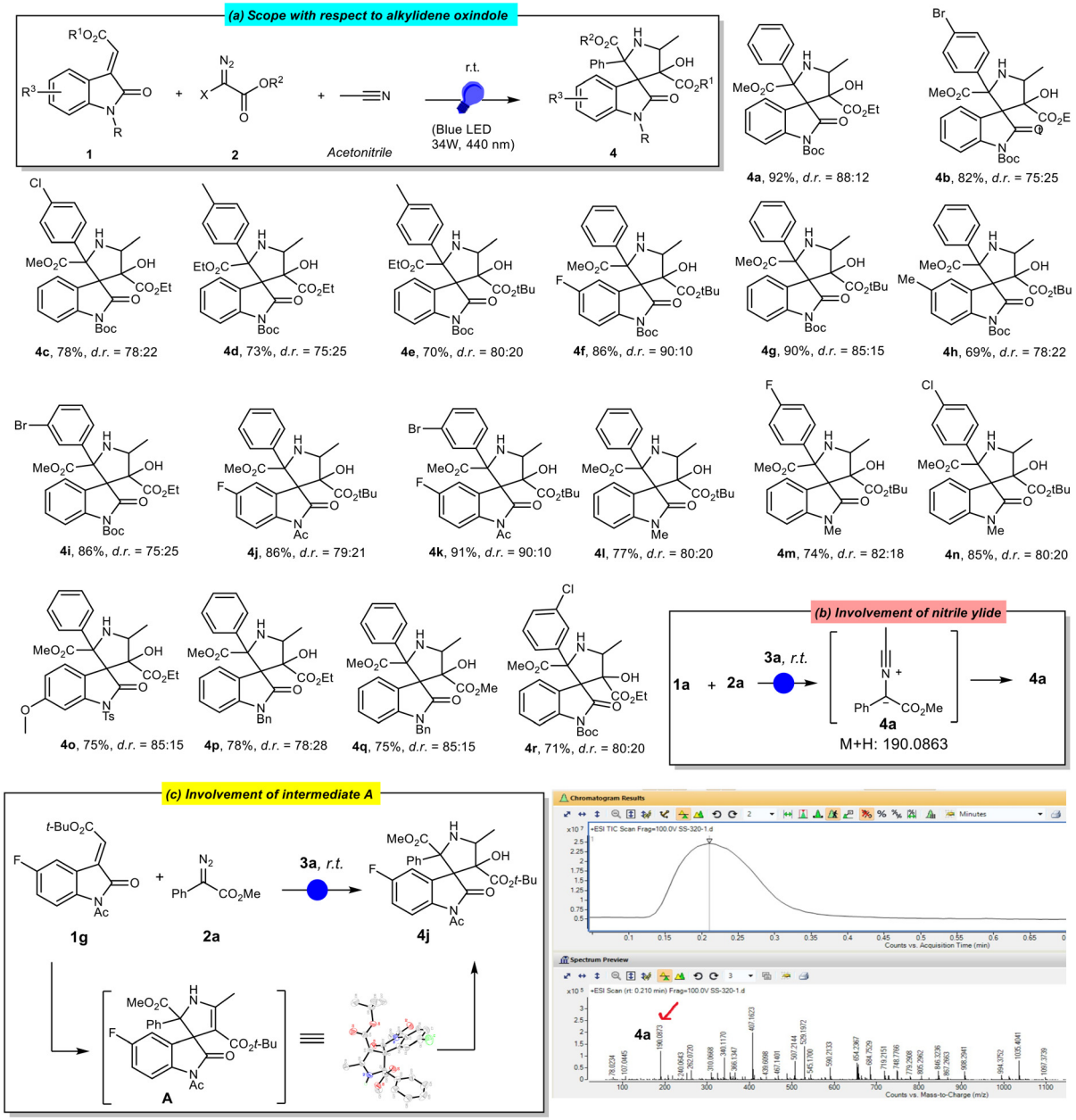

Scheme 2 The generic library of spiropyrrolidine-3,3′-oxindole **4a** → **4r**.

2a in acetonitrile was monitored by LCMS-QTof and the mass spectrum clearly indicated the formation of the nitrile ylide **3a** (Scheme 2b). At the same time, isolating intermediate **A** from the reaction mixture of **1g** with **2a** and **3a** (Scheme 2c) and confirming its structure by single crystal X-ray indicate putatively the formation of the final product **4j** as well as the relative stereochemistry between the quaternary carbon centre adjacent to the pyrrolidine nitrogen and the quaternary carbon at the spiro junction. Additionally, the 2D-NOESY spectrum of the final representative compound **4i** recorded in $CDCl_3$ indicated a through-space ^1H–^1H coupling between the methyl (CH_3) group and the hydroxyl (OH) proton (refer to Scheme S7†). This Nuclear Overhauser Effect (NOE) suggests that the CH_3 and OH protons are spatially close, supporting their proximity within the molecule's 3D conformation. This observation helps to establish the relative stereochemistry of the building block **4**.

Next, we developed a novel one-pot mechanochemical protocol for the synthesis of densely functionalized 2′-aryl-2′,4′-dihydrospiro[indoline-3,3′-pyrazol]-2-one **8** *via in situ* generation of nitrile imines **7** from ethyl diazoacetate **5** and aryl diazonium tetrafluoroborates **6**, followed by their 1,3-dipolar cycloaddition with alkylidene oxindoles **1**. As a model system, we selected *N*-methyl alkylidene oxindole **1m**, ethyl diazoacetate **5a**, and 4-bromophenyl diazonium tetrafluoroborate **6a** in a 1 : 1 : 1 stoichiometric ratio to investigate the formation of

the desired 2′-aryl-2′,4′-dihydrospiro[indoline-3,3′-pyrazol]-2-one derivative **8a** (see ESI Table S1† and Table 2).

Initial solvent screening at room temperature identified dichloromethane (DCM) as the optimal medium, affording **8a** in 61% yield (Table S1,† entry 6). Elevating the temperature to 50 and 70 °C expedites the completion of the limiting reagent **1m**; however the overall yield decreased to ~35% and 40% respectively (Table S1,† entries 7 and 8). Increasing the equivalents of **5a** (2 and 4 eq.) and **6a** (2 eq.) led to an enhanced yield of 72% (Table S1,† entries 9 and 10). Notably, under solvent-free ("neat") conditions, **8a** was obtained in 68% yield with increased amounts of **5a** and **6a**, as depicted in entry 10 (Table S1,† entry 11). These preliminary reactions required an average reaction time of 8–10 hours.

Motivated by the promising outcome under neat conditions and with the goal of enhancing sustainability, we systematically optimized the reaction parameters under solvent-free mechanochemical ball-milling conditions using a Retsch MM400™ high-frequency mixer mill (see ESI Fig. S5†). A series of variables including jar material, ball type/size/number, milling frequency, and duration were thoroughly examined (Table 2).

Initial milling of the reactants in a 10 mL yttria-stabilized zirconia (ZrO_2-Y) jar with a single 10 mm ball at 30 Hz afforded **8a** in 60% yield within 90 minutes (Table 2, entry 1). Reducing the ball diameter to 7 mm and increasing the number of balls to 2 and 3, respectively, improved both the reaction kinetics and yield (65% in 75 min and 60 min, respectively; Table 2, entries 2 and 3). Further enhancement was achieved by increasing the milling frequency. At 70 Hz, the reaction completed in just 30 minutes with no compromise in yield (75%, Table 2, entry 5). Finally, employing a stainless steel (ss) jar equipped with three 7 mm stainless steel balls at 70 Hz furnished **8a** in 81% yield within 30 minutes (Table 2, entry 6). These were deemed the optimal conditions for the mechanochemical synthesis of 2′-aryl-2′,4′-dihydrospiro[indoline-3,3′-pyrazol]-2-one **8**.

With the optimized reaction conditions established, the substrate scope was subsequently investigated using a diverse set of electronically varied alkylidene oxindoles **1m–1s** for their spirocyclization with ethyl and methyl diazoacetate **5a**/**5b** and aryl diazonium tetrafluoroborates **6a–6i** (Scheme 3). The *N*-methyl-substituted alkylidene oxindoles **1m–1p** (ESI Fig. S1†) underwent smooth spirocyclization with **5a** and various aryl diazonium salts **6a–6h**, affording the desired 2′-aryl-2′,4′-dihydrospiro[indoline-3,3′-pyrazol]-2-ones **8a–8j** in commendable yields ranging from 76% to 87%, with moderate diastereoselectivities (dr = 7 : 3 to 8.5 : 1.5), irrespective of the electronic nature of the substituents on **6** (Scheme 3).

Similarly, the *N*-tosyl-substituted alkylidene oxindole **1q** reacted efficiently with *meta*-trifluoromethyl **6g** and *para*-chlorophenyl diazonium tetrafluoroborates **6h** to furnish the corresponding 2′-aryl-2′,4′-dihydrospiro[indoline-3,3′-pyrazol]-2-one derivatives **8k** and **8l** in 79% and 76% yields, respectively, with comparable diastereomeric ratios (dr = 6 : 4). Notably, the *N*-unsubstituted alkylidene oxindoles **1r** and **1s** also participated effectively in the spirocyclization, delivering products **8j**, **8m** and **8n** in moderate yields and diastereoselectivity (dr ≈ 70 : 30 → 85 : 15). As a demonstration for the late-stage functionalisation of drugs, benzocaine, a topical anaesthetic, pain and itch reliever, was converted to its corresponding diazonium salt **6i** and was reacted under the optimized conditions to afford the desired dimethyl 2′-(4-(ethoxycarbonyl)phenyl)-1-methyl-2-oxo-2′,4′-dihydrospiro[indoline-3,3′-pyrazole]-4′,5′-dicarboxylate **8o** in 71% yield (Scheme 3). Finally, 7-chloro and 7-methoxy alkylidene oxindoles **1t** and **1u** afforded the desired products **8p** and **8q** in 75 and 77% yields, respectively, when reacted with **5b** and **6h** (Scheme 3).

Table 2 Optimization of the mechanochemical reaction conditions

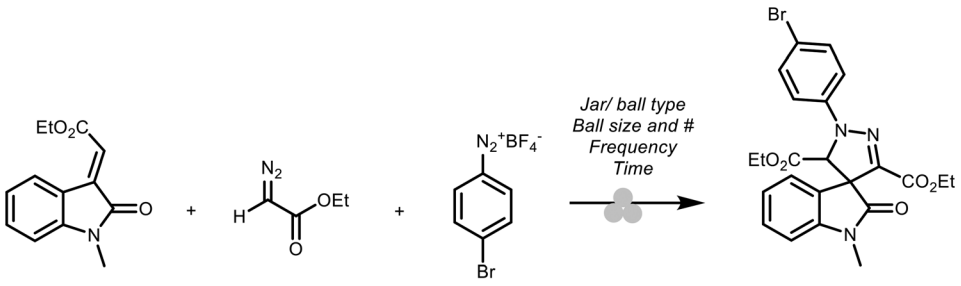

1m 5a 6 8a

Entry	Material of the jar and ball	Ball size and number	Frequency and time	Yield[a]
1	ZrO_2-Y	∅ 10 mm, 1	30 Hz, 90 min	60%
2	ZrO_2-Y	∅ 7 mm, 2	30 Hz, 75 min	65%
3	ZrO_2-Y	∅ 7 mm, 3	30 Hz, 60 min	65%
4	ZrO_2-Y	∅ 7 mm, 3	50 Hz, 45 min	68%
5	ZrO_2-Y	∅ 7 mm, 3	70 Hz, 30 min	75%
6	ss	∅ 7 mm, 3	70 Hz, 30 min	81%

[a] Isolated yield after column chromatography.

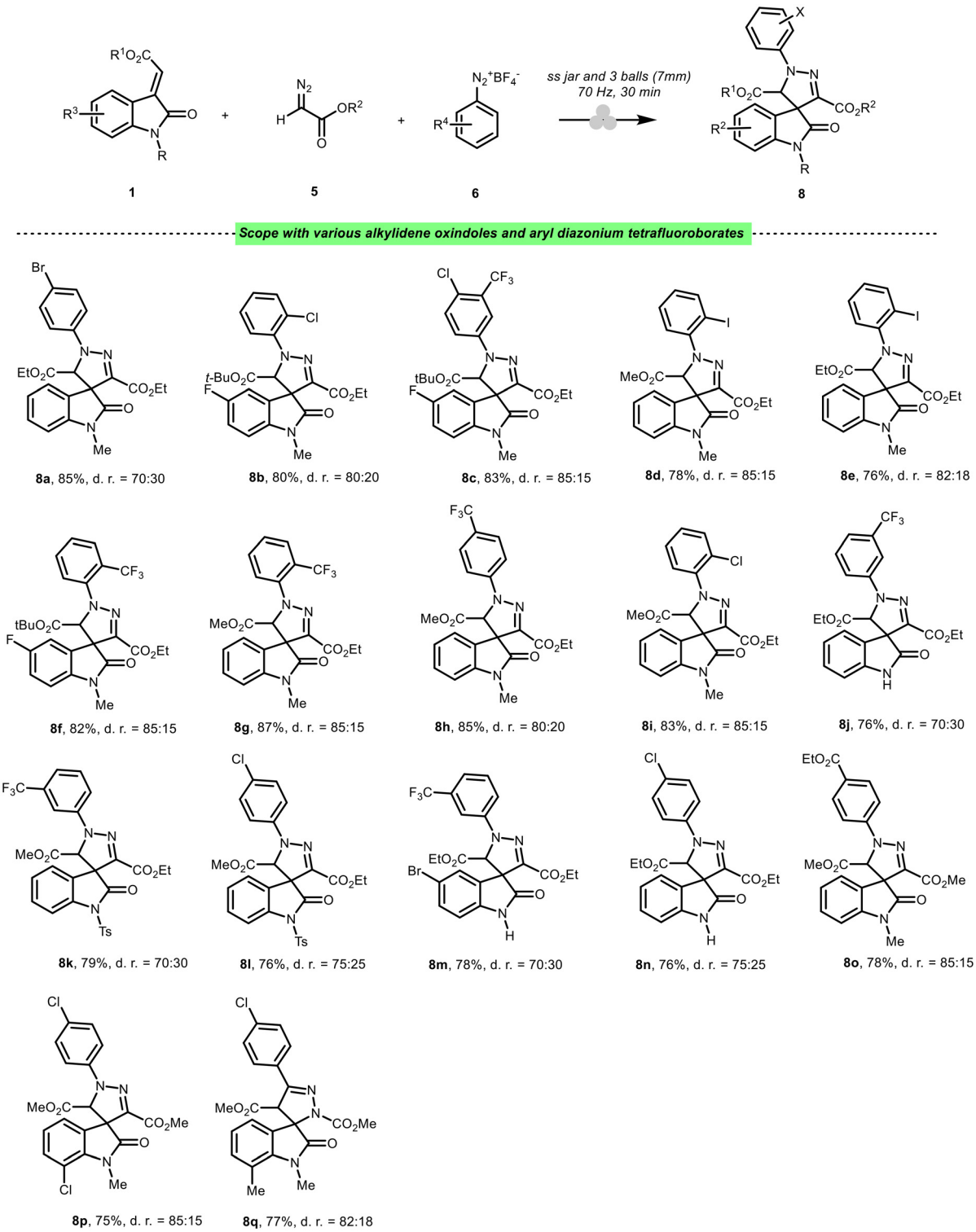

Scheme 3 The generic library of 2′-aryl-2′,4′-dihydrospiro[indoline-3,3′-pyrazol]-2-one, **8a** → **8q**.

This mechanochemical approach thus offers a green and efficient protocol for the synthesis of structurally complex and densely functionalized 2′-aryl-2′,4′-dihydrospiro[indoline-3,3′-pyrazol]-2-ones under mild, catalyst-free conditions.

In a bid to evaluate the scalability of our mechanochemical protocol, we investigated the synthesis of 2′-aryl-2′,4′-dihydrospiro[indoline-3,3′-pyrazol]-2-one **8r** using the DYNO®-MILL (DM) bead milling machine, a horizontal agitator bead mill

used commonly under industrial settings. In spite of its diverse usage for pigment dispersion, pharmaceutical processing, and nanoparticle fabrication, the application of DYNO®-MILL in mechanochemical organic reactions under dry or minimal solvent conditions is limited (Table 3).[31]

A representative scale-up experiment involved milling alkylidene oxindole **1v** (10 mmol), diazonium salt **6a** (20 mmol), and **5b** (40 mmol) under dry conditions using 0.5 mm yttria-stabilized zirconia (ZrO_2/Y_2O_3) DYNO®-BEADS as grinding media. The milling was performed at 5000 rpm, corresponding to approximately 66% of the maximum rotor speed of the DYNO®-ACCELERATOR, with the optimized stoichiometric ratios reported in Table 2. This process provided 2′-aryl-2′,4′-dihydrospiro[indoline-3,3′-pyrazol]-2-one **8r** in 44% isolated yield after 120 minutes (Table 3, entry 1). Considering a nominal handling loss during recovery of the product from the instrument, the actual yield may vary slightly.

Next, we systematically evaluated the milling parameters, *viz* rotor speed and bead filling volume. Decreasing the rotor speed to 4000 rpm resulted in an increased yield of 66% (Table 3, entry 2), while further reduction of the speed to 3000 rpm did not prove detrimental, maintaining a yield of 65% (Table 3, entry 3). These results suggest that 3000 rpm balances optimally between energy input and reaction efficiency for this system.

While optimizing the rotor speed, the filling degree of the reactor chamber with grinding media was also assessed. Decreasing the bead fill to 45% v/v could have enhanced the frequency of bead-particle collisions; subsequently, a significantly improved yield of approximately 75% of **8r** in 35 minutes was observed (Table 3, entry 4). The grinding media type and size were held constant throughout all experiments to ensure reproducibility. Further reduction of the filling degree to 20% v/v led to a decrease in the yield of **8r** (Table 3, entry 5).

These findings indicate that the efficiency of reactions in bead milling is governed not only by chemical stoichiometry but also by mechanical factors such as the rotor speed, bead packing density and quantity, and milling time. The successful scale-up of the solvent-free DYNO®-MILL process highlights the practical viability of this method—comparable reaction time for scale-up (35 minutes) while maintaining comparable yields. It demonstrates the potential to transition bench-scale mechanochemical techniques into industrially relevant batch or continuous-flow systems, providing a greener, more energy-efficient pathway for synthesizing complex heterocycles.

To gain insight into the reaction mechanism, a series of control experiments were conducted (Scheme 4). First, the reaction of **1a**, **5a**, and **6a** under the optimized conditions was carried out in the presence of 2 equivalents of either 2,2,6,6-tetramethylpiperidine-1-oxyl (TEMPO) or butylated hydroxytoluene (BHT). Notably, the reaction proceeded efficiently in both cases, affording the desired products in 75% and 79% yields, respectively (Scheme 4A[1]). These results suggest that the transformation likely follows an ionic, rather than a radical, pathway.

Next, to probe the formation of a nitrile imine intermediate, a trapping experiment was performed using *N*-ethyl maleimide in place of **1a** under otherwise identical conditions. The reaction between **5a**, **6a**, and *N*-ethyl maleimide led to the formation of compound **9**, a fused maleimide–pyrazoline hybrid, in 74% yield (Scheme 4A[2]). This outcome supports the *in situ* formation of nitrile imine species in the reaction.

Based on the control experiment in Scheme 4A[2], we propose that nitrile imine **7** forms *in situ* and undergoes a [3 + 2] cycloaddition with alkylidene oxindole **1**. To evaluate the feasibility of the two possible regioselective pathways

Table 3 Scale-up synthesis of azaindazole **6a** using the bead mill DYNO®-MILL

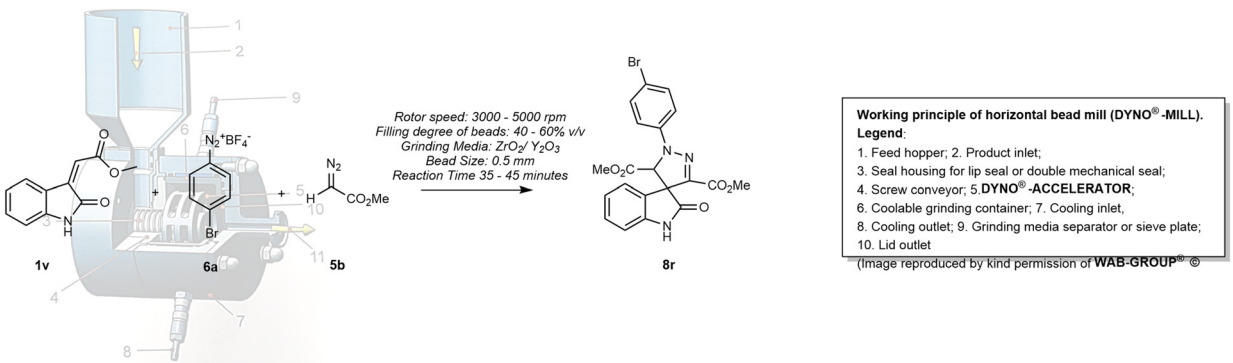

Entry	Rotor speed	Filling degree of beads	Time (minutes)	Yield[a] (%)
1	5000 rpm	60 v/v	120	44
2	4000 rpm	60 v/v	88	66
3	3000 rpm	60 v/v	48	65
4	3000 rpm	45 v/v	35	75
5	3000 rpm	20 v/v	120	25

[a] Isolated yield.

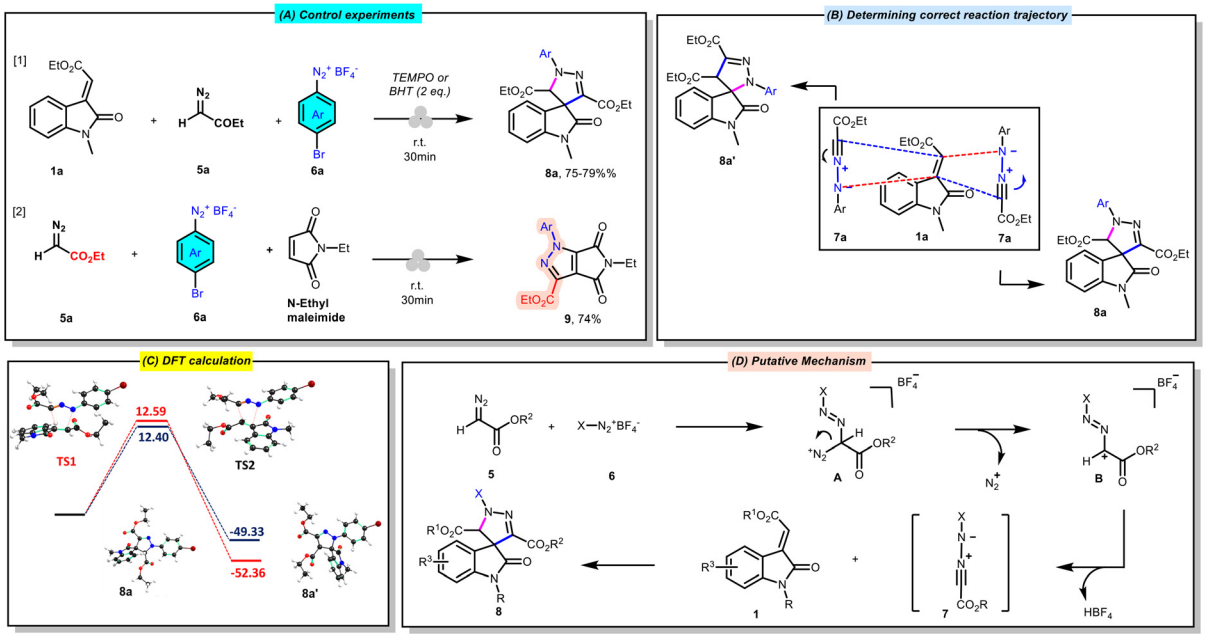

Scheme 4 (A) Control experiments to ascertain the mechanism of 2′-aryl-2′,4′-dihydrospiro[indoline-3,3′-pyrazol]-2-one, **8**. (B) Assessing correct trajectory in the [3 + 2] cycloaddition between *in situ* nitrile imine **7** and **1**. (C) Density functional theory calculations to ascertain the mode of attack. (D) Putative mechanism for the formation of **8**.

(Scheme 4B), we conducted density functional theory calculations (M06-2X/def2-SVP) to model the cycloaddition between **1** and **7**. The results (Scheme 4C) show that both pathways have comparable activation barriers, but the formation of regioisomer **8a** is thermodynamically favoured, with a more negative reaction free energy (−52.3 kcal mol^{-1}) than that of **8a′** (−49.3 kcal mol^{-1}).

Based on the results of the control experiments and supported by DFT calculations (Scheme 4A–C), a plausible reaction mechanism is proposed for the mechanochemical synthesis of 2′-aryl-2′,4′-dihydrospiro[indoline-3,3′-pyrazol]-2-one **8** (Scheme 4D). The key intermediate in this process is the nitrile imine **7**, which is generated *in situ* from the reaction between alkyl diazo acetate **5** and aryl diazonium tetrafluoroborates **6** *via* intermediate **A**. The conversion of **A** to **B** occurs with the extrusion of nitrogen gas (N_2↑), followed by decomposition of **B** through the elimination of HBF_4 to afford nitrile imine **7**. This reactive intermediate then undergoes a [3 + 2] cycloaddition with the alkylidene oxindole **1**, furnishing the desired product **8** (Scheme 4D).

Conclusion

In conclusion, we have developed an efficient and sustainable strategy for the synthesis of spirocyclic oxindole frameworks *via* photochemical and mechanochemical spirocyclization of alkylidene oxindoles **1** under completely additive-free conditions, avoiding the use of acids, bases, or metal catalysts. The photochemical protocol, employing blue LED irradiation, enables the *in situ* generation of nitrile ylides **3** from aceto-nitrile and aryl diazoacetates **2**, which subsequently undergo [3 + 2] cycloaddition and oxidation with **1** to afford spiro[pyrrolidine-3,3′-oxindoles] **4**. In parallel, the mechanochemical approach facilitates the solvent-free generation of nitrile imines **7** from ethyl diazoacetate **5** and aryl diazonium tetrafluoroborates **6** *via* ball milling, enabling the diastereoselective construction of 2′-aryl-2′,4′-dihydrospiro[indoline-3,3′-pyrazol]-2-one **8**.

This dual activation platform not only underscores the versatility of diazo precursors under complementary reaction conditions but also exemplifies an environmentally benign route to access two pharmaceutically relevant spirocyclic scaffolds, widely recognized for their prevalence in bioactive natural products and drug-like molecules.

Conflicts of interest

There are no conflicts to declare.

Data availability

The data supporting this article have been included as part of the ESI.†

Acknowledgements

The authors would like to thank Shiv Nadar Institution of Eminence (Deemed to be University) for funding and support

for Ms. Swetha Singh and Mr. Roopam Pandey. S.S. would like to thank Willy A. Bachofen AG (WAB, Switzerland), in the persons of Erich Ermel and Jan Parduhn, for the loan of DYNO®-MILL system adapted for mechanochemical applications.

References

1 S. S. Panda, A. S. Girgis, M. N. Aziz and M. S. Bekheit, Spirooxindole: A Versatile Biologically Active Heterocyclic Scaffold, *Molecules*, 2023, **28**, 618–649.
2 C. Marti and E. M. Carreira, Construction of Spiro[pyrrolidine-3,3′-oxindoles] – Recent Applications to the Synthesis of Oxindole Alkaloids, *Eur. J. Org. Chem.*, 2003, 2209–2219.
3 A. Monteiro, L. M. Goncalves and M. M. Santos, Synthesis of novel spiropyrazoline oxindoles and evaluation of cytotoxicity in cancer cell lines, *Eur. J. Med. Chem.*, 2014, **79**, 266–272.
4 S. Hati, S. Tripathy, P. Dutta, R. Agarwal, R. Srinivasan, A. Singh, S. Singh and S. Sen, Spiro[pyrrolidine-3, 3′-oxindole] as potent anti-breast cancer compounds: Their design, synthesis, biological evaluation and cellular target identification, *Sci. Rep.*, 2016, **6**, 32213–32222.
5 Á. A. Kelemen, G. Satala, A. J. Bojarski and G. M. Keserű, Spiro[pyrrolidine-3,3′-oxindoles] and Their Indoline Analogues as New 5-HT6 Receptor Chemotypes, *Molecules*, 2017, **22**, 2221–2246.
6 Â. Monteiro, L. M. Gonçalves and M. M. M. Santos, Synthesis of novel spiropyrazoline oxindoles and evaluation of cytotoxicity in cancer cell lines, *Eur. J. Med. Chem.*, 2014, **79**, 266–272.
7 L. R. Raposo, A. Silva, D. Silva, C. Roma-Rodrigues, M. Espadinha, P. V. Baptista, M. M. M. Santos and A. R. Fernandes, Exploiting the antiproliferative potential of spiropyrazoline oxindoles in a human ovarian cancer cell line, *Bioorg. Med. Chem.*, 2021, **30**, 115880.
8 X-H. Chen, Q. Wei, S-W. Luo, H. Xiao and L-Z. Gong, Organocatalytic Synthesis of Spiro[pyrrolidin-3,3′-oxindoles] with High Enantiopurity and Structural Diversity, *J. Am. Chem. Soc.*, 2009, **131**, 13819–13825.
9 D-Z. Chen, W-J. Xiao and J-R. Chen, Synthesis of spiropyrazoline oxindoles by a formal [4 + 1] annulation reaction between 3-bromooxindoles and in situ-derived 1,2-diaza-1,3-dienes, *Org. Chem. Front.*, 2017, **4**, 1289–1293.
10 A. R. Liandi, A. H. Cahyana, D. N. Alfariza, R. Nuraini, R. W. Sari and T. P. Wendari, Spirooxindoles: Recent report of green synthesis approach, *Green Synth. Catal.*, 2024, **5**, 1–13.
11 E. P. J. Janulis, S. R. Wilson and A. J. Arduengo III, The synthesis and structure of a stabilized nitrilium ylide, *Tetrahedron Lett.*, 1984, **25**, 405–408.
12 G. Sicard, A. Baceiredo and G. Bertrand, Synthesis and reactivity of a stable nitrile imine, *J. Am. Chem. Soc.*, 1988, **110**, 2663–2664.
13 C. Escolano, M. D. Duque and S. Vázquez, Nitrile Ylides: Generation, Properties and Synthetic Applications, *Curr. Org. Chem.*, 2007, **11**, 741–772.
14 C. M. Nunes, I. Reva and R. Fausto, Capture of an Elusive Nitrile Ylide as an Intermediate in Isoxazole–Oxazole Photoisomerization, *J. Org. Chem.*, 2013, **78**, 10657–10665.
15 X. Chen, H. Chen, X. Ji, H. Jiang, Z-J. Yao and Hong Liu, Asymmetric One-Pot Sequential Mannich/Hydroamination Reaction by Organo- and Gold Catalysts: Synthesis of Spiro[pyrrolidin-3,2′-oxindole] Derivatives, *Org. Lett.*, 2013, **15**, 1846–1849.
16 G. Yue, Y. Wu, Z. Dou, H. Chen, Z. Yin, X. Song, C. He, X. Wang, J. Feng, *et al.*, Synthesis of spiropyrrolidine oxindoles via Ag-catalyzed stereo- and regioselective 1,3-dipolar cycloaddition of indole-based azomethine ylides with chalcones, *New J. Chem.*, 2018, **42**, 20024–20031.
17 A. Deepthi, N. Acharjee, S. L. Sruthi and C. B. Meenakshy, An overview of nitrile imine based [3 + 2] cycloadditions over half a decade, *Tetrahedron*, 2022, **116**, 132812.
18 M. E. Filkina, D. N. Baray, E. K. Beloglazkina, Y. K. Grishin, V. A. Roznyatovsky and M. E. Kukushkin, Regioselective Cycloaddition of Nitrile Imines to 5-Methylidene-3-phenylhydantoin: Synthesis and DFT Calculations, *Int. J. Mol. Sci.*, 2023, **24**, 1289.
19 G. Utecht-Jarzyńska, K. Nagła, G. Mlostoń, H. Heimgartner, M. Palusiak and M. A. Jasiński, Beilstein, Substituted nitrogen-bridged diazocines, *J. Org. Chem.*, 2021, **28**, 1509–1517.
20 A. S. Girgis, S. S. Panda, A. M. Srour, A. Abdelnaser, S. Nasr, Y. Moatasim and O. Kutkat, , *et al.*, 3-Alkenyl-2-oxindoles: Synthesis, antiproliferative and antiviral properties against SARS-CoV-2, *Bioorg. Chem.*, 2021, **114**, 105131–105148.
21 P. Soam, D. Mandal and V. Tyagi, Divergent and Selective Synthesis of 3-Alkylidene Oxindoles Using Pd-Catalyzed Multicomponent Reaction, *J. Org. Chem.*, 2023, **88**, 11023–11035.
22 S-H. Huang, I-T. Chen and J.-L. Han, Asymmetric (3 + 3) and (4 + 2) Annulation Reactions of 2,3-Dioxopyrrolidines with 3-Alkylidene Oxindoles to Construct Diverse Chiral Heterocyclic Frameworks, *J. Org. Chem.*, 2024, **89**, 8970–8984.
23 H. Huang, Y. Zhang, Q. Du, C. Zheng, C. Jin and S. Li, Synthesis and Antimicrobial Activity of 3-Alkylidene-2-Indolone Derivatives, *Molecules*, 2024, **29**, 5384.
24 N. A. Lozinskaya, E. N. Bezsonova, M. Dubar, D. D. Melekhina, D. R. Bazanov, A. S. Bunev, *et al.*, 3-Arylidene-2-oxindoles as Potent NRH:Quinone Oxidoreductase 2 Inhibitors, *Molecules*, 2023, **28**, 1174.
25 A. Rossetti, A. Sacchetti, M. Bonfanti, G. Roda, G. Rainoldi and A. Silvani, Metal-free visible-light-promoted intermolecular [2 + 2]-cycloaddition of 3-ylideneoxindoles, *Tetrahedron*, 2017, **73**, 4584–4590.
26 H. Qiu, H. Srinivas, P. Zavalij and M. P. Doyle, Unprecedented Intramolecular [4 + 2]-Cycloaddition between a 1,3-Diene and a Diazo Ester, *J. Am. Chem. Soc.*, 2016, **138**, 1808–1811.
27 L. Zhou, M. P. Doyle, L. Zhou and M. P. Doyle, Lewis Acid Catalyzed Indole Synthesis via Intramolecular Nucleophilic

Attack of Phenyldiazoacetates to Iminium Ions, *J. Org. Chem.*, 2009, **74**, 9222–9224.

28 K. O. Marichev, F. G. Adly, A. M. Carranco, E. C. Garcia, H. Arman and M. P. Doyle, Catalyst Choice for Highly Enantioselective [3 + 3]-Cycloaddition of Enoldiazocarbonyl Compounds, *ACS Catal.*, 2018, **8**, 10392–10400.

29 I. D. Jurberg and H. M. L. Davies, Blue light-promoted photolysis of aryldiazoacetates, *Chem. Sci.*, 2018, **9**, 5112–5118.

30 C. Bao-Gui, Y. Wei-Zhong, L. Lei and X. Jun, Visible Light-Promoted Diazoacetates and Nitriles Generating Nitrilium Ions Trapped by Benzotriazoles and Carboxylic Acids, *Org. Lett.*, 2022, **24**(36), 6647–6652.

31 R. Geib, E. Colacino and L. Gremaud, Sustainable Beckmann Rearrangement using Bead-Milling Technology: The Route to Paracetamol, *ChemSusChem*, 2024, **17**(12), e202301921, DOI: **10.1002/cssc.202301921**.